Validation of a stochastic temperature generator focusing on extremes and an example of use for climate change

Sylvie Parey, Thi Thu Huong Hoang, Didier Dacunha-Castelle

Validation of a stochastic temperature generator focusing on extremes and an example of use for climate change

Temperature generator, extremes and climate change

Parey S.*[(1)], Hoang T.T.H. [(1)], Dacunha-Castelle D. [(2)]

1 EDF/R&D, 6 quai Watier 78 401 CHATOU Cedex, France

2 Laboratoire de Mathématiques, Université Paris 11, Orsay, France

Corresponding author : S. Parey Phone : +33 1 30 87 76 14, Sylvie.parey@edf.fr

ABSTRACT :

The paper presents a stochastic Seasonal Functional Heteroscedastic Auto-Regressive model developed to simulate daily (minimum, maximum or mean) temperature time series coherent with observed time series and designed to reliably reproduce extreme values through a careful study of the extremes and their bounded character. The model is first validated using different daily minimum and maximum weather-station time series over Eurasia and the United-States in different climatic regions. It is shown that the model is able to produce coherent results both for the bulk of the distribution and for its extremes and especially that it can produce higher or lower extreme values than observed. Then a possible use in the climate change context is tested. It consists in fitting the model over the first part of a long temperature time series and in using it to simulate a large number of possible trajectories for the second part when temperature has increased. Two approaches have been tested to do so, one based on a simple mean change in mean and variance and the other in considering the full seasonalities and trends estimated over the observed second part of the time series. Both approaches have been found to give good results as well for the bulk as for the extremes of the temperature distribution over the second part of the period. However, the second approach allows taking interannual variability changes into account, which leads to more realistic results when this occurs. These results give confidence in the possibility of using this tool as a statistical downscaling tool reliably reproducing temperature extremes.

Keywords : daily temperature, stochastic modeling, extremes

1. Introduction

Weather generators are commonly used in environmental or financial studies as a way to simulate key properties of observed meteorological records and then produce long series of daily weather parameters. Two main approaches can be found in those developments: weather generators are either based on randomly pooling out analog days in a database of past observations, or on statistically generating the desired variables with a stochastic model whose parameters are estimated on a database of past observations. The advantage of the first approach is a better reproduction of the observed distribution, but the main drawback is that it cannot reproduce non observed values. Although the second approach is based on parametric or semi-parametric definitions of the distributions, its main advantage is its ability to produce physically realistic unobserved situations. This second approach is preferred here as the focus is on extreme events. Most efforts in weather generator developments have been devoted to precipitation (see Wilks & Wilby 1999 for a review). Precipitation is namely a crucial parameter in many environmental studies and its representation is complicated by its intermittent nature. Here again, different approaches can be found. Cowpertwait et al. (2007) propose a model of storm cells whose occurrence follows a Poisson process and during which rain cells occur as a secondary Poisson process. Other generators are based on different daily states, from the simple dry and wet days to more sophisticated weather type definitions, possibly introduced as a hidden state variable using Hidden Markov Models (Ailliot et al. 2008; Sansom & Thompson 2010). Then, following Richardson (1981), weather generators are developed to represent simultaneously precipitation and other variables like temperature (daily minimum and maximum), solar radiation or wind, for use in agricultural studies essentially. Such models are increasingly used to downscale global climate model results in impact studies (Wilks 1992, Semenov & Barrow 1997, Wilks &Wilby 1999, Hansen 2002, Kysely & Dubrovsky 2005, Semenov 2008) because they allow taking variability change into account. The interest in extremes further motivates the use of such models; however they generally must be improved to adequately reproduce extreme events (Furrer & Katz 2008). Semenov (2008) showed that if precipitation extremes are reasonably well represented by a Richardson type generator (called LARS-WG) temperature extremes are generally not, because the normality assumption used for the residuals is not universally true. Even with the use of weather types and skewed normal distributions (WACS-Gen), Flecher et al. (2010) recognize having difficulties in reproducing extreme events.

Stochastic temperature models are also used in the framework of weather derivatives. Weather derivative products provide protections against “weather risk", that is against the unpredictable component of weather fluctuations, called "weather surprises," or "weather noise." This thus necessitates some knowledge on this "weather noise" over space and time, which motivated the development of stochastic models (Campbell & Diebold 2005, Mraoua & Bari 2007, Benth & Saltyte-Benth 2011).

Extreme events are important for industrial adaptation, for installations design as well as for their running. Our goal is then to propose a temperature generator able to correctly reproduce temperature extremes. The general principle of such stochastic models, whatever their usage, consists in modeling the temperature (daily maximum or minimum or mean) as the summation of a deterministic part and a stochastic process, designed to represent the random fluctuations around the mean:

$X(t) = \Lambda(t) + \Phi(t)Z(t)$, where $\Lambda(t)$ and $\Phi(t)$ are deterministic and $Z(t)$ stochastic. $\Lambda(t)$ contains at least a seasonal component, and usually also a trend component. $\Phi(t)$ is most often 1. The stochastic part generally presents an autoregressive structure, more or less sophisticated: from an AR1 (first order autoregressive) to a GARCH (General Autoregressive Conditional Heteroscedastic).

For the proposed model, our basic idea comes from a preliminary analysis of the correlations and especially from the shape of the conditional variance of $Z(t)$ when $Z(t-1)$ is fixed. In particular, this conditional variance drastically decreases outside of a bounded interval. This leads to the use of a FARCH (Functional AutoRegressive conditional Heteroscedastic) model, the simplest one able to take this behavior into account. FARCH processes are the first order Euler scheme approximation of the discrete Markov chain given by the sequence of discrete observations of a diffusion. Furthermore, the coefficients (drift and diffusion) of the diffusion are those of the FARCH process. Thus we are led to consider temperature as a continuous time process with continuous trajectories. If $X(t)$ can be assumed as Markovian then the continuous time process is a diffusion. The Markovian property can be tested. This mathematical justification is coherent with the physical interpretation of the heat equation as a diffusion of the thermal energy but also with more general considerations on non linearity and stochasticity which can be found in Sura (2012). The building of the model is based on discrete temperature observations at a given time interval, for instance every day, and the diffusive property has to be translated in this restrictive framework. The obtained SFHAR (Seasonal Functional Heteroscedastic AutoRegressive) model, with careful treatment of the extreme upper and lower bounds, is described in details in Dacunha-Castelle et al. (2013) and briefly reviewed in the appendix. The present paper focuses on the validation of the model for different climates in Eurasia and in the United-States and proposes a possible application in the climate change context. The model is calibrated on temperature time series starting in 1950 for the United States and Eurasia. It simulates the residuals after accounting for seasonalities and trends in mean and variance.

After a brief description of the model and the presentation of the used temperature time series in section 2, section 3 is devoted to the validation of the model for different climates. Then, in section 4, the model is calibrated on the first part of the observed time series, and then, different strategies are tested and validated to simulate the second part, warmer in average than the first one. Discussion and perspectives are proposed in section 5.

2. Model and observations

In the following, X(t) is the observed temperature time series (either daily minimum or daily maximum temperature), m(t) its mean trend, $S_m(t)$ the seasonality of the mean, $s^2(t)$ its variance trend, $S_v(t)$ the seasonality of the variance and Z(t) the modeled residual time series.

2.1 Brief description of the model

2.1.1 Pre-processing

As stated before, the model is designed to simulate the residuals Z(t) from a temperature time series X(t) after accounting for seasonalities ($S_m(t)$ and $S_v(t)$) and trends (m(t) and s(t)) in mean and standard deviation. The first step is then to identify and remove these deterministic parts from X(t) to obtain Z(t). This is done through the following succession of steps:

1) Estimation of the seasonality of X(t): $\hat{S}_m(t)$
2) Estimation of the trend $\widehat{m}$(t) from the time series $(X(t) - \hat{S}_m(t))$
3) Estimation of the seasonality of the variance from $\left[X(t) - \hat{S}_m(t) - \widehat{m}(t)\right]^2$: $\hat{S}_v^2(t)$

4) Estimation of the trend $\hat{s}^2(t)$ from the time series $\left[X(t) - \hat{S}_m(t) - \hat{m}(t)\right]^2 / \hat{S}_v(t)$

5) Finally, $\hat{Z}(t) = \dfrac{X(t) - \hat{S}_m(t) - \hat{m}(t)}{\hat{S}_v(t)\hat{s}(t)}$

Quantities over headed by a hat correspond to estimations. The identification of seasonality is based on the fitting of a trigonometric function of the form: $\theta_0 + \sum_{i=1}^{p}(\theta_{i,1}\cos\frac{2\pi t}{365} + \theta_{i,2}\sin\frac{2\pi t}{365})$, and the number p of trigonometric terms is chosen through an Akaike criterion. This parametric identification has been compared to the non parametric STL method (Seasonal Trends decomposition, Cleveland et al. 1990) and both approaches have been found very similar.

The trend identification is conducted in a non parametric way by using the LOESS technique (Local regression, Stone 1977). The LOESS estimator is obtained by locally fitting a d^{th} degree polynomial to the data via weighted least squares. Throughout this work, the local linear fit is used, which means d = 1. This method implies the choice of a smoothing parameter, which controls the balance between goodness of fit to the data and smoothness of the regression function. The smoothing parameter is obtained through an automated selection. This selection is difficult here as the data are correlated, non stationary and heteroscedastic. The modified partitioned cross-validation technique proposed in Hoang (2010) is used. It is based on the classical partitioned cross-validation technique of Marron (1987): the observations are partitioned into g subgroups by taking every g^{th} observations, for example the first subgroup consists of the observations 1,1 + g,1 + 2g,..., the second subgroup consists of the observations 2,2+g,2+2g,.... The observations in each subgroup are then independent for high g. Chu & Marron (1991) define the optimal asymptotic bandwidth for Partitioned Cross-Validation in the case of constant variance as $h_{PCV} = h_0 g^{1/5}$, with h_0 estimated as the minimiser of $PCV_g(h) = \frac{1}{g}\sum_{k=1}^{g} CV_{0,k}(h)$ ($CV_{0,k}$ is the ordinary Cross-Validation score for the k-th group). This approach has been modified to take heterocedasticity into account. Then, the optimal g corresponds to the minimum of a more complicated expression (Hoang 2010) and in practice, it is preferred to estimate h_{MPCV} (the optimal bandwidth of the Modified Partitioned Cross Validation) for different values of g and to retain the values of g for which

h_{MPCV} is not too bad (that is not too close to zero and not higher than 0.7). For each g the trends m and s are estimated by LOESS with bandwidth $\hat{h}^g_{MPCV}$ to obtain an estimator of the expression to minimize. The value of g corresponding to the minimum value is retained, giving the corresponding optimal bandwidth h_{MPCV}.

The order of estimation of seasonality and trend is not important, it has been checked that estimating trends then seasonality leads to similar results for Z(t).

The procedure is illustrated in figure 1.

Careful studies of Z(t) have shown that although seasonality has been removed from the mean and variance, some seasonality remains in the higher order moments like skewness and kurotsis of Z(t) and in its autocorrelations. However, no significant remaining trends could have been found in high order moments, autocorrelations or extremes of Z(t).

2.1.2 Model for Z(t)

The proposed model is described in detail in Dacunha-Castelle et al. (2013) and summarized in the appendix. The first step is to estimate the extremes of Z(t). The upper and lower bounds r_1 and r_2, together with the corresponding shape parameters ξ_1 and ξ_2 are estimated by fitting a GEV distribution to the minima and the maxima of Z(t) respectively. The extremes of Z(t) do not show any clear seasonality and the fitting is done with 73-day blocks (5 blocks per year). Sensitivity tests on the choice of block length showed that the results do not significantly differ. The shape parameter is negative, thus the distributions are bounded. However, if it is too close to 0, the simulation may be problematic. If this happens, it is advised to slightly change the block length in order to get a better estimate of this parameter.

Then the proposed model is justified. It consists of a modification of a Seasonal Functional Heteroscedastic AutoRegressive model of the form:

$Z(t) = bZ(t-1) + a(t, Z(t-1))\varepsilon_t$, ε_t being a normal distribution with 0 mean and unit variance, and:

$b = \theta_0 + \sum_{j=1}^{p_1}(\theta_{j,1}\cos\frac{2\pi t}{365} + \theta_{j,2}\sin\frac{2\pi t}{365})$, p_1 being chosen by an Akaike criterion, because seasonality remains in the autocorrelation, and a is estimated as a degree 5 trigonometric polynomial:

$$a^2(t,Z(t-1)) = (\hat{r}_2 - t)(t-\hat{r}_1)\sum_{k=0}^{5}\sum_{j=1}^{p_2}(\alpha_{1,k}^{j}\cos\frac{2\pi t}{365} + \alpha_{2,k}^{j}\sin\frac{2\pi t}{365})Z(t-1)^k$$

under constraints $(a^2)'(r_1) = \frac{2b(r_1)}{1-\frac{1}{\xi_1}}$; $(a^2)'(r_2) = \frac{2b(r_2)}{1-\frac{1}{\xi_2}}$ and $a^2(t) > 0 \forall t$, with p_2 chosen by an Akaike criterion, r_1 and r_2 being respectively the lower and upper bound of the extreme value distributions of Z(t) and ξ_1 and ξ_2 the corresponding shape parameters. The form of *a* and the constraints are given by the extreme value theory of the continuous time process (Davis 1982). In practice, the autoregressive part of Z(t) is first estimated, then *a* is estimated from $(Z(t)-\hat{b}Z(t-1))^2$ by maximum likelihood with constraints.

Once the parameters have been estimated, as many sequences of Z(t) as desired can be simulated with the model. A sequence consists of a certain number of years and each day t, Z(t) is computed from Z(t-1). The initial value is randomly selected from the observed residuals. A condition is added to insure that each Z(t) remains inside the limit bounds r_1 and r_2: if the simulated value at time t exceeds the upper bound or is lower than the lower bound, it is disregarded and another value for Z(t) is computed from Z(t-1). This is equivalent to a modified model where the distribution of ε_t is a truncated normal distribution whose truncation depends on the value of Z(t-1) (its values are $\frac{r_1 - b\mathrm{Z(t-1)}}{a(\mathrm{Z(t-1)})}$ and $\frac{r_2 - b\mathrm{Z(t-1)}}{a(\mathrm{Z(t-1)})}$). Thus the obtained simulated residuals are bounded.

Then a simulation of the initial temperature time series is obtained by re-introducing the estimated deterministic parts $\hat{S}_m(t), \hat{m}(t), \hat{S}_v(t)\ and\ \hat{s}(t)$. As an indication, 100 simulations of a 60-year daily time series need around 7mn of computing time on a standard laptop.

Compared to most generators found in the literature, our model differs in its bounded property and in the careful retrieval of the smoothing parameter to compute the non parametric trends in both mean and variance to obtain the then simulated residuals. The main consequence is thus that the simulated time series' length is at most that of the observed one used to determine the trends. But as many equivalent time series as desired can be computed, giving a similarly rich sample. The optimal smoothing parameter is linked to interannual variability, which allows an indirect consideration of this property of temperature time series besides daily variance. Furthermore, the auto-correlations are fully seasonal and the behavior of the extremes is carefully introduced in the volatility (or lag 0 auto-correlation) coefficients $a(t)$. This is expected to really improve the ability of the model at reproducing extremes, which will be examined in this paper.

2.2 Observed time series

The validation of the model is conducted for different climates in Eurasia and in the United-States. For Eurasia, weather station time series of daily minimum temperature (TN) and daily maximum temperature (TX) are obtained from the ECA&D project database. The project gives indications of homogeneity through the results of different break identification techniques (Klein Tank et al. 2002). First, the series which could be considered as homogenous (stated as "useful" in the database) over the period1950-2009 have been selected for both TN and TX. Then, only the time series with less than 5% missing data are kept, leading to 106 series for TX and 120 for TN (many TX series, mostly in Russia, have missing values from 2007 onward whereas the corresponding TN ones have missing values only in 2009).

For the United States, weather station TX and TN time series are obtained from the Global Historical Climatology Network – Daily Database (GHCN daily) (Menne et al. 2011). A similar selection procedure left us with 86 series for TX and 85 for TN.

Among these time series, 4 weather stations corresponding to different climates, in terms of mean annual temperature, have been chosen for each continent, as listed in table 1. As stated before, the weather station of Olekminsk in Russia cannot be considered for TX as it exhibits too many missing values. No other station with a similar climate to that of Olekminsk is available for TX.

3. Validation

For each of the 7 (for TX) or 8 (for TN) temperature time series, the parameters of the model are fitted over the whole period length. Then, 100 simulations of the model are computed for each location and the results are compared to the observed time series both for the representation of the bulk of the distribution and of its warm and cold extremes.

3.1 Bulk of the distribution

Table 2 and 3 summarize the comparison of the mean, variance, skewness and kurtosis of the distributions of each temperature time series obtained from the observations and from the 100 model simulations (mean value and 95% confidence interval). The results show that these different moments of the observed distribution of daily maximum or minimum temperature are correctly reproduced by the stochastic simulations, although the higher moments are sometimes less accurately reproduced. This good result may be linked to the domination of the annual cycle, thus the seasonal distributions have been compared too. Figure 2 shows the Q-Q plots of observed and simulated winter and summer distributions of TN in Olekminsk and TX in Death Valley. Similar results for the other stations confirm that the model reasonably reproduces the seasonal temperature distributions.

Figure 3 shows that the mean annual cycle, as well as that of the standard deviation, is faithfully represented. Figure 3 is for TN in Berlin and TX in Jacksonville, but similar results are found for each individual time series.

Kolmogorov-Smirnov tests have been applied to compare the distributions obtained for each day of the year between observations on the one hand and simulations on the other hand, and they show that the distributions can be considered as similar with a 95% confidence level. The proposed stochastic model is thus able to correctly reproduce the bulk of the daily minimum or maximum temperature distributions for different climates.

3.2 Extremes

The model is constructed for a bounded variable and the simulations are made in such a way that each simulated value remains inside the estimated bounds of the residuals. Thus first, the Generalized Extreme Value (GEV) distribution parameters for the simulated residuals are compared to those of the observed ones, both for the lowest and the highest extremes. Figure 4 shows the distributions for each parameter (location μ, scale σ and shape ξ) obtained from the 100 simulations for the highest (warm) extremes (upper panels) and the lowest (cold) extremes (lower panel) together with the same parameters obtained from the observed residuals (red line) for TN in Berlin and TX in Death Valley. The results show, and this is true for the other temperatures and locations too, that the shape parameter is generally better reproduced in the simulations than the location and scale parameters. It can be mathematically proven that the proposed stochastic model is able to produce the correct shape parameter when a truncated normal distribution is used for ε_t.

Then table 4 compares the 50-year Return Levels (RL) of the maxima of TX and the minima of TN for the different locations over the whole observation period. The estimation is made by fitting a GEV to the block maxima of summer TX or winter TN (Coles 2001) with the maximum likelihood method and considering the choice of 2 blocks per season as a reasonable bias / variance compromise. The estimation is conducted as if the extremes would not present trends over the entire period, which is of course wrong, but it simplifies the computations and is sufficient to give a first view of the representation of the extremes by the proposed model. For each of the 100 simulations, the 50-year RL is computed. The given confidence interval is obtained as the 2.5th and 97.5th percentiles of the distribution of the 100 RLs, whereas for the observations the confidence interval is the 95% one given by the delta-method (that is based on the asymptotic normality of the maximum likelihood estimators). Generally, the simulations give higher warm RLs and lower cold RLs than observed, but the confidence intervals obtained from the observations generally show some overlapping with the 2.5th and 97.5th percentiles of the distribution obtained from the simulations (except for TX in Glasgow and TN in Petropavslosk). The fact that the model produces higher (or lower for cold temperature) extremes than observed is not surprising because the simulations produce 100 possible realities, among which higher or lower extremes could have been observed. This thus shows that the model is not only able to produce extremes, but also to produce more extreme extremes than observed, which is interesting.

Finally, the ability of the model to produce heat or cold waves has been investigated. Cold waves are defined as periods of consecutive days with daily minimum temperature lower than the 2nd percentile and heat waves as periods of consecutive days with daily maximum temperature above the 98th percentile. The number of consecutive days varies between 1 and 15 days, the last class corresponding to the few episodes with more than 15 days, if any. Thus for each location the 2nd and 98th percentiles of the observed time series are computed and the distribution of episodes in the observed time series is compared to the minimum, maximum and mean frequencies of such a distribution in the 100 simulations. Figure 5 shows the results for cold waves in Petropavslovsk and heat waves in Charleston. Even though the stochastic model tends to overestimate the proportion of 1-day cold excursions compared to the observations, it is still able to produce longer episodes in a reasonable proportion, even the longest ones. This tendency to overestimate the frequency of 1-day events is less systematic for heat waves.

4. Possible use in the climate change context

The previous section has shown that the proposed stochastic model, when fitted on a temperature time series, is able to correctly reproduce the bulk of the distribution as well as the extremes of the studied time series. This is an interesting result as far as the model allows reliable simulations of a high number of possible temperature evolutions at a given location giving access to potential unobserved but still possible levels. In the climate change context, it could also be very interesting to produce possible temperature evolutions for the future, given that climate is warming. General or regional climate models are designed to allow such projections for the different climatic variables, but their ability to represent extreme values for a precise location is still questionable. Thus different downscaling techniques, from simple bias corrections to full dynamical downscaling with limited area models, are explored (Maraun et al. 2010). The aim here is to check whether the proposed stochastic model can be used as a statistical downscaling tool giving reliable indications on temperature extremes.

4.1 Simulation procedure

To do so, among the previously used temperature time series, two have been selected as showing an identifiable break in the evolution of mean temperature, splitting the time series in two sub-series of roughly similar length. Break is identified using the Mudelsee (2009) method which consists in selecting the date for which the standard deviation of the residuals resulting from the two-phase regression model is the minimum, after having considered all dates (except the first and last 5 ones, to avoid edge effects) as potential break points. This simple technique is used because the identification of the break is not the ultimate goal of the work but is only made for the sake of illustration. More general regression techniques exist, such as the segmented regression proposed by Muggeo (2003). Such a break is identified in year 1980 for TN in Berlin and in year 1985 for TX in Death Valley for both the mean and variance evolutions.

Then, each time series is split into two shorter time series: 1950-1980 and 1981-2009 for TN in Berlin and 1962-1985 and 1986-2009 for TX in Death Valley. For both sub series, the residuals Z(t), after removing trends and seasonalities in mean and variance, are estimated. The parameters of the stochastic model defined to simulate Z(t) are fitted over the first sub-series in each case. Then, the reconstruction of the desired temperature time series for each period necessitates that trends and seasonalities are added to the simulated residuals. Two ways are compared to compute the desired temperature time series over the second (and warmer) sub period:

1) Average mean and variance changes are added to the trends computed from the first sub period: if m_1 is the mean over the first period, s_1 the standard deviation, and m_2 and s_2 the same quantities for the second period: $X_2(t) = \hat{S}_{m_1}(t) + \hat{m}_1(t) + (m_2 - m_1) + \hat{S}_{v_1}(t) * \hat{s}_1(t) * \frac{s_2}{s_1} * Z(t)$, where $\hat{S}_{m_1}(t), \hat{m}_1(t), \hat{S}_{v_1}(t)$ *and* $\hat{s}_1(t)$ are the seasonalities and trends estimated over the first sub period. Table 5 summarizes the means and variances of each sub series.
2) Seasonalities and trends are those computed over the second sub period: $X_2(t) = \hat{S}_{m_2}(t) + \hat{m}_2(t) + \hat{S}_{v_2}(t) * \hat{s}_2(t) * Z(t)$ where $\hat{S}_{m_2}(t), \hat{m}_2(t), \hat{S}_{v_2}(t)$ *and* $\hat{s}_2(t)$ are the seasonalities and trends estimated over the second sub period.

In the first way, interannual variability, included in the smoothing parameter of the non parametric trends, remains that of the first period, whereas the second approach allows taking interannual variability of the second period into account.

4.2 Results

4.2.1 Bulk of the distribution

As previously, the first comparisons aim at validating the reproduction of the main characteristics of the bulk of the distribution. Table 6 gives the observed and simulated mean and variance obtained for the second period in winter and in summer with each of the used approach for each location and variable. As expected, approach 2, which takes trends and seasonalities of the second period into account, gives better results, but the results given by the first approach are close to the observations too. Figure 6 gives a better view of the entire distribution: it presents, for different percentiles (from the very low 1% to the very high 99% through the median), the distribution of such percentiles obtained from the 100 simulations in black and the values obtained from the observations in red. It shows that for all percentiles, the observed estimates fall inside the distributions of the simulated estimates, whatever the approach taken for the simulations. This thus validates the two approaches to compute the distribution of temperature for a future period when mean and variance have changed.

4.2.2 Extremes

Let us now look at the extremes, in terms of 50-year return levels and of heat or cold waves. Table 7 gives the obtained 50-year return levels for period 2, again in considering the series as stationary, and estimated from the observations and from each type of simulation. As in the previous section, the 95% confidence interval for the observations is computed with the delta-method while for the simulations, the 2.5th and 97.5th percentiles of the distribution of the estimated 100 50-year RLs are taken. The results show that for Berlin, approach 2 gives slightly better results than approach 1 whereas for Death Valley this is not the case. This can be explained by the fact that the smoothing parameter computed to estimate the mean and variance trends is the same for both periods for Death Valley (0.08) whereas for Berlin it changes from 0.32 in the first period to 0.08 in the second one. Thus, in Berlin, interannual variability for daily minimum temperature is higher in the second period, and taking this into account logically improves the simulations. Figure 7 shows the distributions of cold waves in Berlin and heat waves in Death Valley according to each simulation procedure in the same way as figure 5 in the previous section. Here, both approaches give similarly good results.

5 Conclusion and perspectives

In this paper, a stochastic Seasonal Functional Heteroscedastic Auto-Regressive model for daily temperature has been presented and validated for different climates in Eurasia and in the United States.

First, it has been shown that when fitted over a long temperature series (daily minimum or maximum) and used to simulate a large number of equivalent trajectories, the model is able to correctly reproduce both the bulk and the extremes of the observed distribution. In particular, it is able to produce higher or lower extremes than observed.

Then, for two temperature time series for which a break in the evolution of both mean and variance could have been identified around the middle of the period, the model has been constructed over the first part of the period and used to reproduce the second part. As the model simulates the residuals after accounting for trends and seasonalities in mean and variance, the reconstruction of the observed variable for any period consists in re-introducing this information on trends and seasonalities. Two approaches have been tested: firstly taking global mean and variance changes between both periods into account (like in the so-called “delta method”) and secondly introducing the real trends and seasonalities computed over the second period. The second approach allows taking interannual changes into account if any occurs. This is the case for the daily minimum temperature time series in Berlin and then, this last approach improves the results. Both approaches however give equivalently good results, both in terms of bulk of the distribution as in terms of extremes.

This sounds encouraging in the perspective of using this tool as a downscaling technique suitable to deal with temperature extremes. The second approach particularly, opens the possibility of taking possible interannual variability changes into account. We can imagine for example that the model is fitted over an observed temperature time series representative of a location of interest and then, future temperatures for this location can be obtained by introducing the seasonalities and trends estimated over a corresponding, suitably corrected, grid point time series produced by different climate models with different scenarios.

Present results show that this technique is able to give reliable information for the temperature extremes, for highest or lowest values as well as episodes. However, further studies will be devoted to hot and cold episodes. Although the model is able to produce long cold or heat waves, it should be able to produce more of such events among 100 simulations. Here the autocorrelation coefficient has been considered periodic, but it is suspected that it may increase once a certain high or low threshold is crossed. This will be further investigated. In a broader perspective, the model could be part of a more general weather generator in addition with a rainfall generator for example.

Appendix: model description

Before choosing a model for the reduced process Z(t), after removal of trends and seasonalities in mean and variance, its correlations and conditional variance have been analyzed. The non parametric analysis of the conditional variance of Z(t) given Z(t-1) shows a particular behavior: linear in the core of the distribution, close to zero for very high and low values of Z(t-1), the conditional mean being close to a linear function. The first idea is thus to choose a FARCH model with finite bounds for the distribution. The application of the extreme theory is not justified at this step (because a mathematical theory does not exist for these processes) but it gives, once done, a negative shape parameter ($\xi < 0$) that suggests a bounded distribution.

The idea is then to choose a modified FARCH model $Z(t) = b(Z(t-1)) + a(Z(t-1))\varepsilon_t$ where ε_t is a truncated Gaussian noise whose bounds depend on the value of Z(t-1). The second step is then to represent the temperature as a continuous time process (with continuous trajectories). The FARCH processes are the first order Euler scheme approximation of the discrete Markov chain M, where M(t) is the observation at time t of the continuous diffusion given by: $dY(t) = b(t, Y(t)) + a(t, Y(t))dW(t)$ where *b* is the drift, *a* the diffusion coefficient and W(t) a Brownian motion. The estimation of the coefficients of such a continuous stationary diffusion is commonly done using its first order Euler scheme Z, thus a FARCH process with the same functional coefficients. Technically this situation is very informative in relation with the extremes theory. From the geometric ergodicity of the diffusion, the extreme parameters and the bounds of the continuous time process can be estimated using only the chain M. Z is from now considered as an approximation of M. Now we use the continuous process as a tool. The extremes coefficients and thus the bounds r_1 and r_2 are estimated by fitting a GEV distribution to the maxima of the reduced series here modeled as M(t). The support of M(t), say (r_1,r_2), is bounded so that r_1 and r_2 are inaccessible boundary points for Y. At the boundary, we have:

1. *a* and *b* are defined and continuous on $[r_1,r_2]$
2. $b(r_1)b(r_2) \neq 0$

Under hypotheses 1. and 2. and $\xi < 0$, we prove in Dacunha-Castelle et al. (2013) the following theorem:

If the distribution of the maximum of the diffusion Y is in the domain of attraction of a GEV distribution with $\xi < 0$ then the marginal distribution is common to the chain M and to Y and so they are in the same domain of max attraction.

We have the following behavior of *a* as $x \to r_2$:

$$a^2(x) = -2b(r_2)\xi'(r_2 - x) + o(r_2 - x) \quad \text{where} \quad \xi' = \frac{\xi}{\xi - 1}$$

This information is then plugged-in as constraints in the likelihood of the Euler scheme to estimate coefficients *a* and *b* with bound constraints.

Acknowledgements

The authors acknowledge the data providers in the ECA&D project (http://eca.knmi.nl) and in the National Climatic Data Center in NOAA (www.ncdc.noaa.gov). They also would like to thank the reviewers whose proposals helped improving the paper.

References

Ailliot P, Thompson C, Thomson P (2008) Space time modelling of precipitation using a hidden Markov model and censored Gaussian distributions. Journal of the Royal Statistical Society.

Benth EF & Saltyte Benth J (2011) Weather Derivatives and Stochastic Modelling of Temperature. International Journal of Stochastic Analysis.

Campbell SD & Diebold FX (2005) Weather forecasting for weather derivatives. Journal of the American Statistical Association. Vol. 100, N°469, pp 6-16, Applications and case studies, DOI 10.1198/016214504000001051

Cleveland RB, Cleveland WS, Mcrae JE, & Terpenning I. (1990): Stl: a seasonal-trend decompostion procedure based on loess (with discussion). Journal of Official Statistics, 6:3-73.

Chu C K & Marron J S (1991) Comparison of two bandwidth selectors with dependent errors. Annals of Statistics. 19: 1906-1918

Coles S (2001) An introduction to statistical modeling of extreme values, springer series in statistics. Springer Verlag, London

Cowpertwait P, Isham V, Onof C (2010) Point process models of rainfall: developments for fine-scale structure. Proceedings of the Royal Society. A 463, 2569–2587, doi:10.1098/rspa.2007.1889

Dacunha-Castelle D, Hoang TTH, Parey S (2013) Modeling of air temperatures: preprocessing and trends, reduced stationary process, extremes, simulation. Journal of the French Statistical Society, accepted for publication.

Davis RA (1982). Maximum and minimum of one-dimensional diffusions. Stochastic Processes and their applications, 13:1-9.

Flecher C, Naveau P, Allard D, Brisson N (2010) A Stochastic Weather Generator for skewed data. Water Resources Research. Vol. 46, 7, doi:10.1029/2009WR008098

Furrer EM & Katz RW (2008) Improving the simulation of extreme precipitation events by stochastic weather generators. Water Resources Research, Vol. 44

Hansen JW (2002) Realizing the potential benefits of climate prediction to agriculture: issues, approaches, challenges. Agric Syst 74:309–330

Hoang TTH (2010) Modélisation de séries chronologiques non stationnaires, non linéaires: application à la définition des tendances sur la moyenne, la variabilité et les extrêmes de la température de l'air en Europe. PhD thesis work (written in English), http://www.tel.archives-ouvertes.fr/tel-00531549/fr/

Klein Tank AMG et al. (2002) Daily dataset of 20th-century surface air temperature and precipitation series for the European Climate Assessment. International Journal of Climatology 22:1441–1453. Data and metadata available at http://eca.knmi.nl

Kysely J, Dubrovsky M (2005) Simulation of extreme temperature events by a stochastic weather generator: effects of interdiurnal and interannual variability reproduction. International Journal of Climatology 25:251-269

Maraun D, Wetterhall F, Ireson AM, Chandler RE, Kendon EJ, Widmann M., Brienen S., Rust HW, Sauter T, Themeß M., Venema VKC, Chun KP, Goodess CM, Jones RG, Onof C, Vrac M, Thiele-Eich I (2010) Precipitation downscaling under climate change: Recent developments to bridge the gap between dynamical models and the end user, Reviews of Geophysics, 48(3), DOI: 10.1029/2009RG000314

Marron JS (1987) Partitioned cross-validation. Econometric Review, 6 :271-284.

Menne MJ, Durre I, Vose RS (2011) An overview of the Global Historical Climatology Network – Daily Database. Journal of Applied Meteorology and Climatology

Mraoua M & Bari D (2007) Temperature stochastic modelling and weather derivatives pricing: empirical study with Moroccan data. Afrika Statistika. Vol. 2, N°1 pp 22-43

Mudelsee M (2009) Break function regression. The European Physical Journal Special Topics, 174:49-63

Muggeo VMR (2003) Estimating regression models with unknown break-points. Stat. Med., 22, 3055–3071.

Richardson CW (1981) Stochastic simulation of daily precipitation, temperature, and solar radiation. Water Resources Research. 17, 182–90.

Sansom J & Thompson P (2010) A hidden seasonal switching model for high-resolution breakpoint rainfall data. Water Resources Research Water Resources Research. Vol. 46, 8, doi:10.1029/2009WR008602

Semenov MA (2008) Simulation of extreme weather events by a stochastic weather generator. Climate Research. Vol. 35: 203-212

Semenov M. & Barrow EM (1997) Use of a stochastic weather generator in the development of climate change scenarios. Climatic Change 35, 397–414.

Semenov MA & Brooks RJ (1999) Spatial interpolation of the LARS-WG stochastic weather generator in Great Britain. Climate Research. Vol. 11: 137-148

Stone C. J. (1977), Consistent nonparametric regression. Annals of Statistics, 5: 595-620

Sura P (2012) Stochastic Models of Climate Extremes: Theory and Observations. In Extremes in a Changing Climate: Detection, Analysis and Uncertainty, edited by A. AghaKouchak, D. Easterling, K. Hsu, S. Schubert, and S. Sorooshian, Springer, doi: 10.1007/978-94-007-4479-0 2.

Wilks DS (1992) Adapting stochastic weather generation algorithms for climate change studies. Climatic Change, 22: 67-84

Wilks DS & Wilby RL (1999) The weather generation game: a review of stochastic weather models. Progress in physical geography. 23,3 pp 329-357

List of tables

Table 1: presentation of the considered temperature time series: period lengths and mean observed temperature

Table2: mean, variance, skewness and kurtosis estimated from observed and simulated daily maximum temperature (TX) time series. For the simulations, the mean values with the 95% confidence interval in brackets are given.

Table 3: same as table 2 but for daily minimum temperature (TN)

Table 4: 50-year Return Levels (RLs) estimated from observed and simulated time series. For observations, the 95% confidence interval (in brackets) is obtained with the delta-method; for simulations, the given interval corresponds to the 2.5th and 97.5th percentiles of the distribution of the 100 obtained 50-year RLs

Table 5: mean and standard deviation estimated for the first part of the time series (m_1 and s_1) and for the second part (m_2 and s_2). First part corresponds to 1950-1980 for Berlin and 1962-1985 for Death Valley and second part to 1981-2009 for Berlin and 1986-2009 for Death Valley

Table 6: observed and simulated winter and summer mean and variance for the second period (1981-2009 for Berlin, 1986-2009 for Death Valley) according to each of the 2 approaches used to reconstruct temperature (sim1 and sim2: mean with 95% confidence interval in brackets)

Table 7: 50-year Return Levels (RLs) of winter cold TN in Berlin and summer warm TX in Death Valley estimated from observed and simulated time series for the second period (1981-2009 for Berlin, 1986-2009 for Death Valley) and according to both approaches to reconstruct temperature (simulations 1 and simulations 2). For observations, the 95% confidence interval (in brackets) is obtained with the delta-method; for simulations, the given interval corresponds to the 2.5th and 97.5th percentiles of the distribution of the 100 obtained 50-year RLs

List of figures

Figure 1: illustration of the derivation of the residuals from an observed daily temperature time series. The upper panel shows the original time series (top), its seasonality (middle) and trend (bottom) on the left and the time series of variance (top), its seasonality (middle) and trend (bottom) on the right, and the lower panel shows the obtained time series of residuals.

Figure 2: Q-Q plots of the summer and winter distributions for daily minimum temperature in Olekminsk (left panel) and daily maximum temperature in Death Valley (right panel). The solid line materializes the diagonal; the dots are for the mean simulation and the dashed lines for the 95% confidence interval of the simulations

Figure 3: observed (red) and simulated (black: mean –solid line- and 95% confidence interval –dashed line-) mean annual cycle and daily standard deviation

annual cycle for daily minimum temperature in Berlin (top panel) and daily maximum temperature in Jacksonville (bottom panel)

Figure 4: distributions of the parameters of the Generalized Extreme Value (GEV) distribution fitted to the 100 simulations of the residuals (black): warm extremes (top panels: location μ, scale σ and shape ξ from left to right) and cold extremes (bottom panels, same disposition) with their 2.5th and 97.5th percentiles (black dotted lines) and value of the same parameters obtained from the observations (red line). The top panels are for daily minimum temperature in Berlin and the bottom ones for daily maximum temperature in Death Valley.

Figure 5: frequencies of the 1- to more than 15-day long cold waves in Petropavlovsk (top panel) and 1- to more than15-day long heat waves in Charleston (bottom panel). A cold wave is obtained as consecutive days with daily minimum temperature lower than the 2nd percentile of the observations and heat waves as consecutive days with daily maximum temperature higher than the 98th percentile of the observations. The mean frequencies obtained from the simulations are represented by a solid black line, with the minimum and maximum frequencies in dotted black lines and the observed frequencies are represented by solid red lines.

Figure 6: distributions of the 1st, 10th, 50th, 60th, 90th and 99th percentiles of the 100 simulated temperature distributions estimated for daily minimum temperature in Berlin (top panels) over the second period (1981-2009) with the first approach (left panel) and the second approach (right panel), together with the estimation of the same percentiles from the observations over the same period (red line). The bottom panel is similar but for daily maximum temperature in Death Valley over period 1986-2009.

Figure 7: frequencies of the 1- to more than 15-day long cold waves in Berlin (top 2 panels) and 1- to more than 15-day long heat waves in Death Valley (bottom 2 panels). The definitions of cold and heat waves are the same as in figure 5. The mean frequencies obtained from the simulations are represented by a solid black line, with the minimum and maximum frequencies in dotted black lines and the observed frequencies are represented by solid red lines. For each location, the top panel corresponds to the first simulation approach and the bottom one to the second one.

Tables

Table 1

Weather station	Daily minimum temperature TN		Daily maximum temperature TX	
	period	Mean annual mean (°C)	period	Mean annual mean (°C)
Biarritz	1956-2009	10.1	1956-2009	17.7
Berlin	1950-2009	5.1	1950-2009	13.4
Petropavlovsk	1950-2009	-3.3	1950-2009	6.9
Olekminsk	1950-2009	-11.3	-	-
Death Valley	1962-2009	17.0	1962-2009	32.8
Charleston	1950-2009	15.4	1950-2009	23.0
Jacksonville	1950-2009	5.2	1950-2009	17.5
Glasgow	1950-2009	-0.7	1950-2009	12.5

Table 2

	Daily maximum temperature TX							
	mean		variance		skewness		kurtosis	
	obs	sim	obs	sim	obs	sim	obs	sim
Berlin	13.4	13.4 [13.3;13.5]	84.1	83.2 [80.1;85.9]	-0.03	-0.02 [-0.06;0.02]	-0.78	-0.79 [-0.85;-0.72]
Biarritz	17.7	17.7 [17.6;17.8]	37.1	37.2 [35.9;38.7]	0.07	0.05 [-0.01;0.10]	-0.06	-0.23 [-0.33;-0.10]
Petropavlovsk	6.9	6.9 [6.7;7.1]	237.8	238.2 [233.6;243.9]	-0.18	-0.16 [-0.18;-0.13]	-1.03	-1.08 [-1.11;-1.05]
Olekminsk	-	-	-	-	-	-	-	-
Death Valley	32.8	32.8 [32.6;32.9]	112.2	112.2 [109.5;114.8]	-0.08	-0.07 [-0.10;-0.04]	-1.19	-1.17 [-1.21;-1.11]
Jacksonville	17.5	17.4 [17.3;17.6]	137.1	136.3 [133.2;139.7]	-0.43	-0.39 [-0.41;-0.36]	-0.82	-0.87 [-0.91;-0.82]
Glasgow	12.5	12.5 [12.2;12.7]	204.3	202.8 [196.6;208.7]	-0.38	-0.33 [-0.37;-0.30]	-0.59	-0.63 [-0.69;-0.58]
Charleston	23.0	23.0 [22.9;23.1]	50.9	50.7 [49.6;52.0]	-0.46	-0.41 [-0.44;-0.39]	-0.48	-0.57 [-0.63;-0.51]

Table 3

	Daily minimum temperature TN							
	mean		variance		skewness		kurtosis	
	obs	sim	obs	sim	obs	sim	obs	sim
Berlin	5.1	5.1 [5.0;5.2]	49.1	48.5 [46.4;50.9]	-0.36	-0.33 [-0.39;-0.26]	-0.21	-0.28 [-0.48;-0.06]
Biarritz	10.1	10.1 [10.0;10.2]	30.2	30.1 [29.1;31.1]	-0.35	-0.35 [-0.40;-0.31]	-0.30	-0.31 [-0.41;-0.21]
Petropavlovsk	-3.3	-3.3 [-3.4;-3.1]	196.6	196.7 [191.4;202.9]	-0.41	-0.39 [-0.42;-0.37]	-0.85	-0.87 [-0.91;-0.81]
Olekminsk	-11.4	-11.3 [-11.5;-11.1]	335.4	334.9 [325.6;344.7]	-0.30	-0.29 [-0.31;-0.27]	-1.14	-1.13 [-1.17;-1.09]
Death Valley	16.9	16.9 [16.8;17.0]	102.9	102.7 [101.3;104.3]	0.02	0.03 [0.00;0.05]	-1.13	-1.11 [-1.14;-1.09]

Jacksonville	5.2	5.2 [5.0;5.3]	110.0	109.7 [106.3;113.9]	-0.33	-0.31 [-0.35;-0.27]	-0.58	-0.62 [-0.71;-0.53]
Glasgow	-0.7	-0.7 [-0.9;-0.5]	147.1	146.9 [141.1;152.0]	-0.58	-0.54 [-0.58;-0.50]	-0.25	-0.30 [-0.40;-0.19]
Charleston	15.4	15.4 [15.3;15.5]	60.0	60.0 [58.6;61.6]	-0.40	-0.37 [-0.40;-0.34]	-0.86	-0.90 [-0.94;-0.85]

Table 4

	TX		TN	
	observations	simulations	observations	simulations
Berlin	38.2 [37.1;39.2]	39.8 [38.8;41.0]	-23.4 [-25.5;-21.0]	-26.5 [-31.5;-22.9]
Biarritz	39.6 [38.8;40.4]	41.0 [39.0;43.5]	-9.4 [-12.2;-6.6]	-11.0 [-12.6;-9.7]
Petropavlovsk	38.5 [37.6;39.5]	41.5 [39.3;44.8]	-43.7 [-45.2;-42.1]	-48.7 [-52.5;-45.3]
Olekminsk	-	-	-56.3 [-57.8;-54.8]	-58.8 [-61.4;-56.2]
Death Valley	54.3 [53.5;55.1]	55.2 [54.3;56.1]	-6.4 [-7.5;-5.3]	-7.4 [-8.8;-6.0]
Jacksonville	41.8 [40.3;43.3]	43.1 [41.5;44.5]	-29.5 [-31.3;-27.7]	-33.8 [-38.5;-30.6]
Glasgow	42.0 [41.1;42.8]	45.5 [44.3;46.9]	-42.9 [-44.4;-41.4]	-46.9 [-50.4;-44.0]
Charleston	39.5 [38.6;40.4]	40.3 [39.5;41.2]	-11.3 [-13.7;-9.0]	-8.8 [-10.0;-7.5]

Table 5

	m_1 (°C)	m_2 (°C)	s_1 (°C)	s_2 (°C)
TN Berlin	4.7	5.5	7.0	6.9
TX Death Valley	32.3	33.2	10.4	10.7

Table 6

	winter						summer					
	mean			variance			mean			variance		
	obs	sim1	sim2	obs	sim1	sim2	obs	sim1	sim2	obs	sim1	sim2
TN Berlin	-1.7	-2.0 [-2.7; -1.4]	-1.8 [-2.5; -1.2]	25.0	25.2 [20.8; 29.8]	23.2 [18.9; 28.4]	13.1	13.2 [12.9; 13.4]	13.0 [12.8; 13.2]	8.7	8.2 [7.5; 8.9]	9.1 [8.2; 9.9]
TX Death Valley	20.2	20.7 [20.4; 21.1]	20.2 [19.9; 20.6]	18.7	18.2 [15.5; 20.8]	18.4 [15.9; 21.2]	45.7	45.4 [45.1; 45.8]	45.7 [45.3; 46.0]	15.0	13.6 [11.7; 16.1]	14.5 [12.6; 17.1]

Table 7

	observations	simulations 1	simulations 2
Cold extremes Berlin	-21.6 [-24.7;-18.5]	-28.2 [-37.3;-22.3]	-26.7 [-37.5;-21.5]
Warm extremes Death Valley	53.2 [52.2;54.1]	54.3 [53.2;55.6]	55.1 [54.1;56.2]

Figures

Figure1

Seasonality and trends of the mean	Seasonality and trends of the variance
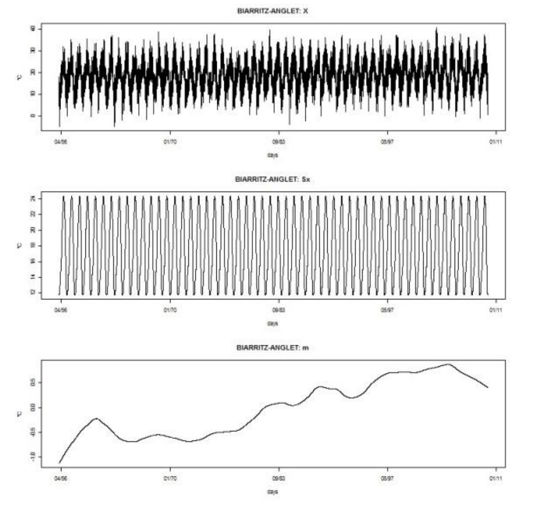	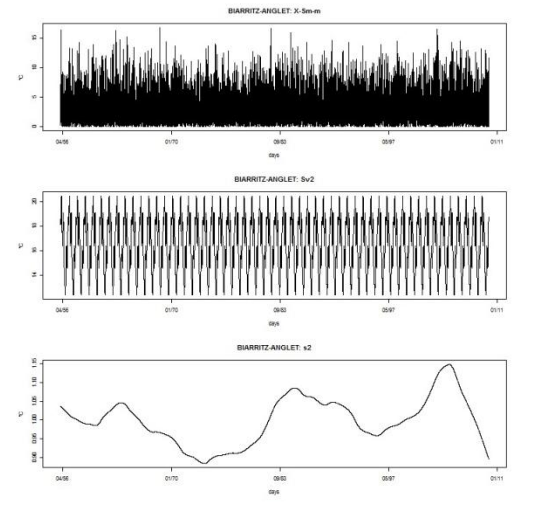

Obtained residuals

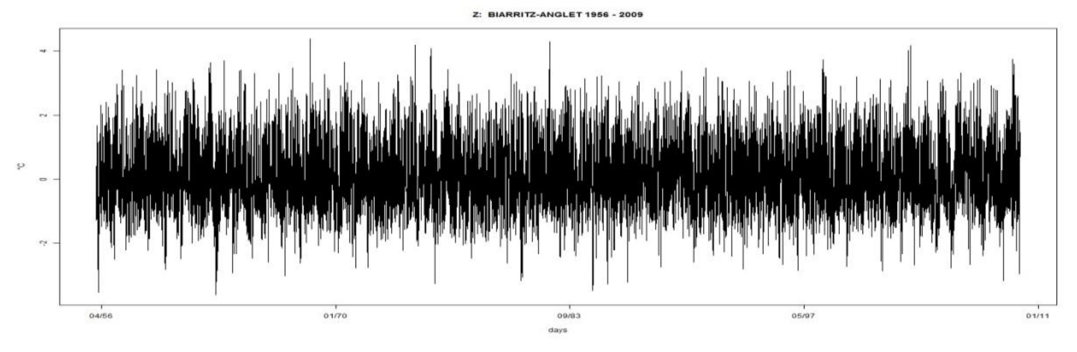

Figure 2

OLEKMINSK daily minimum temperature TN	DEATH VALLEY daily maximum temperature TX

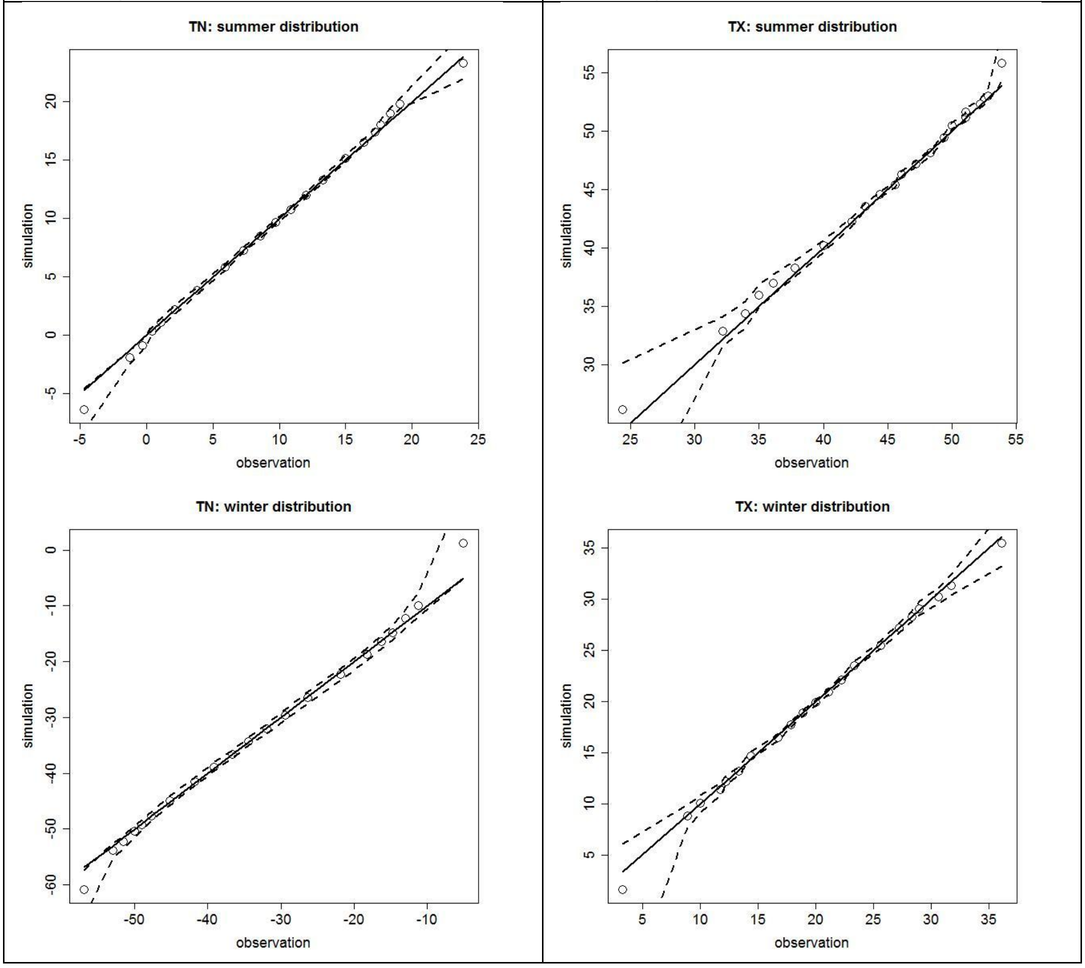

Figure 3

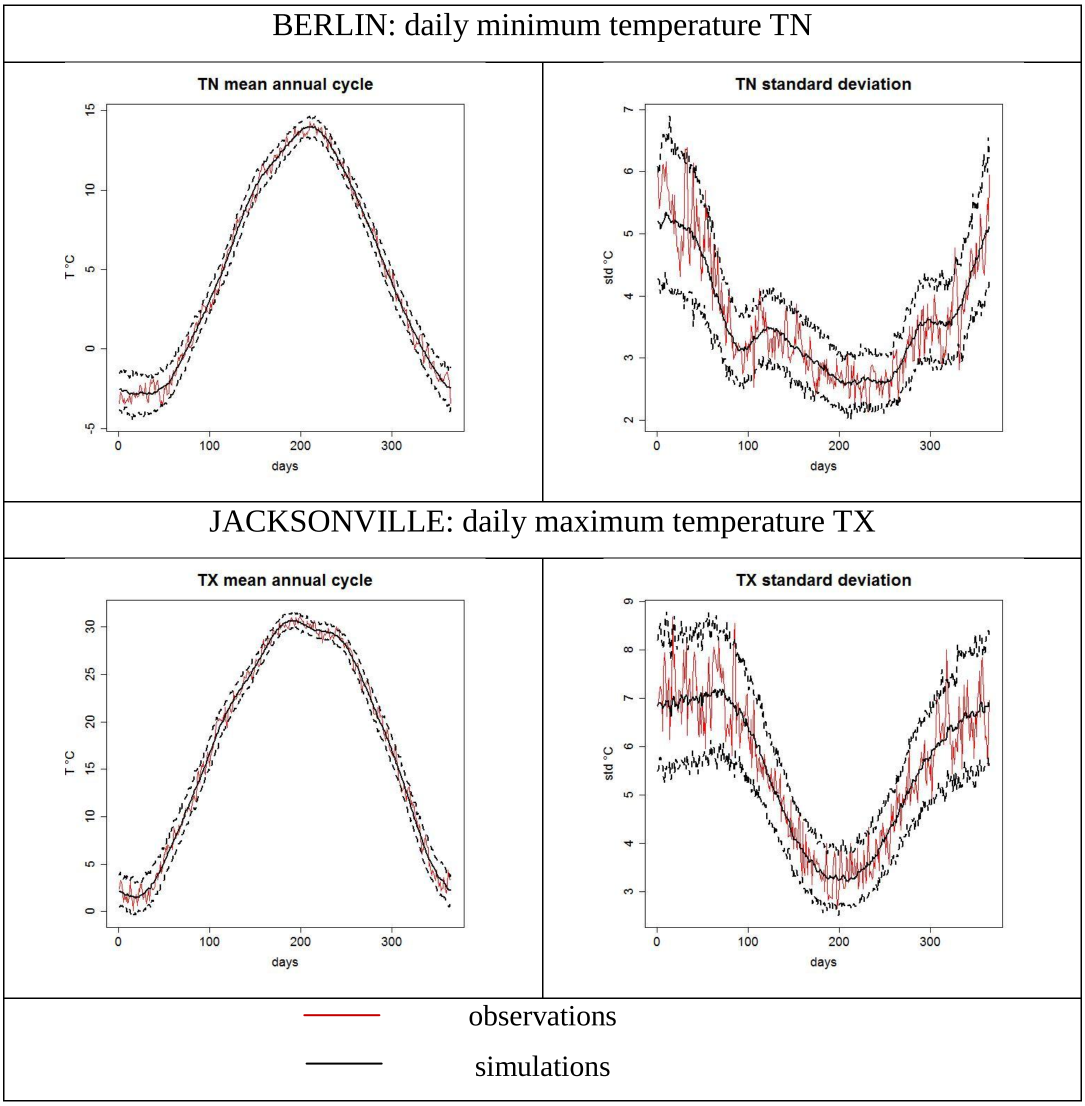
BERLIN: daily minimum temperature TN
TN mean annual cycle
T °C
days
TN standard deviation
std °C
days
JACKSONVILLE: daily maximum temperature TX
TX mean annual cycle
T °C
days
TX standard deviation
std °C
days
observations
simulations

Figure 4

BERLIN: daily minimum temperature TN

Warm extremes

Cold extremes

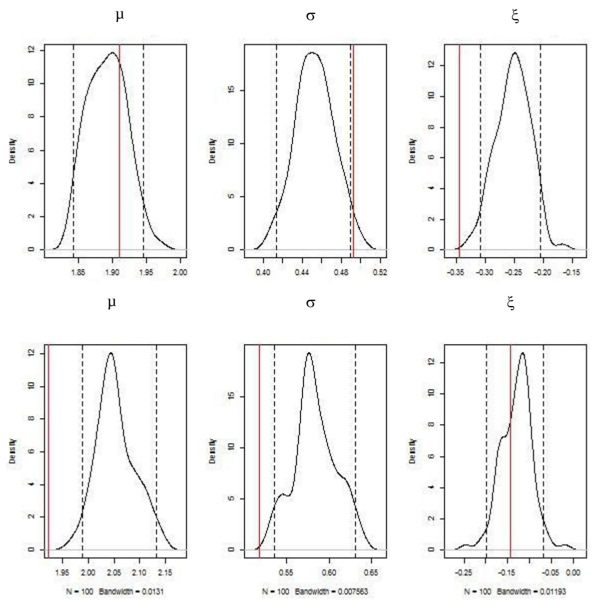

DEATH VALLEY: daily maximum temperature TX

Warm extremes

Cold extremes

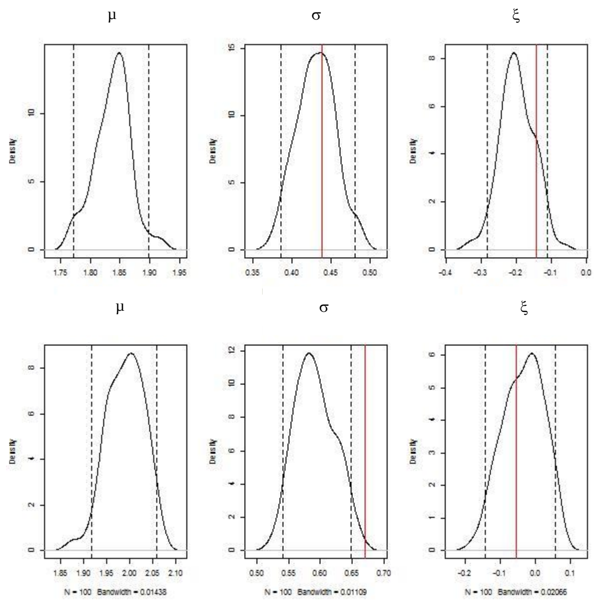

observations

simulations

Figure 5

PETROPAVLOVSK: cold waves distribution

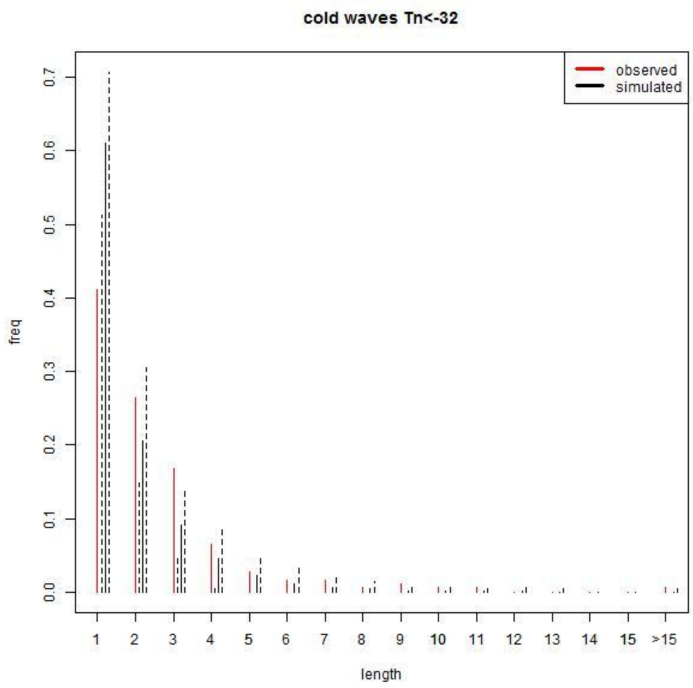

CHARLESTON: heat waves distribution

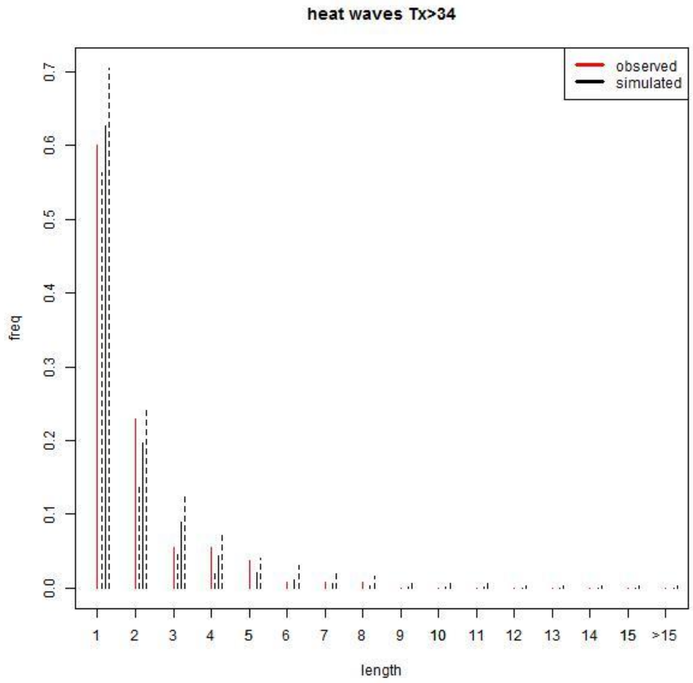

observations

simulations

Figure 6

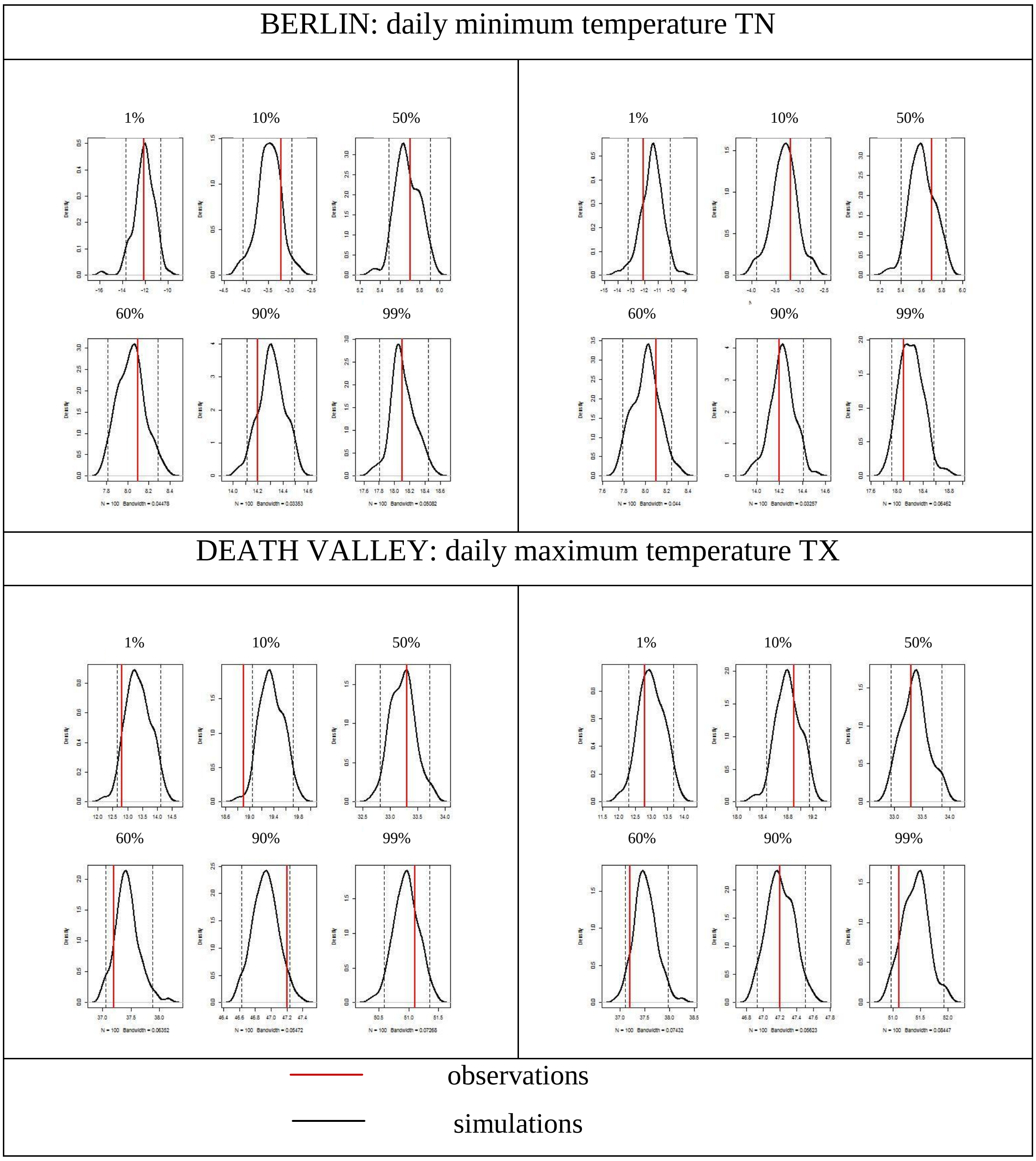
BERLIN: daily minimum temperature TN
1%
10%
50%
60%
90%
99%
DEATH VALLEY: daily maximum temperature TX
observations
simulations

Figure 7

BERLIN: cold waves distribution

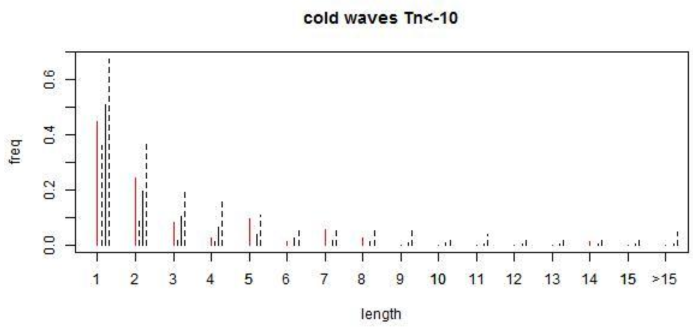

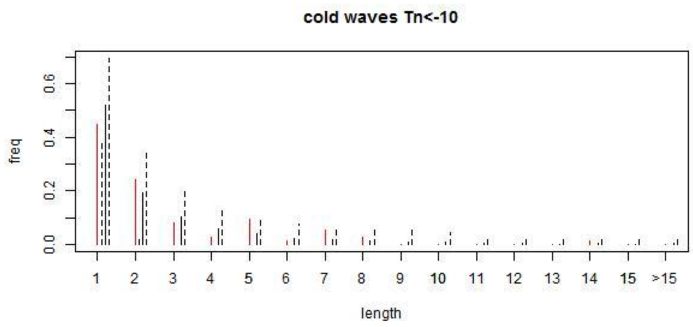

DEATH VALLEY: heat waves distribution

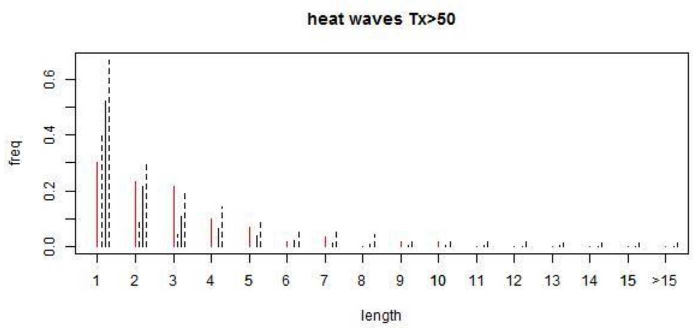

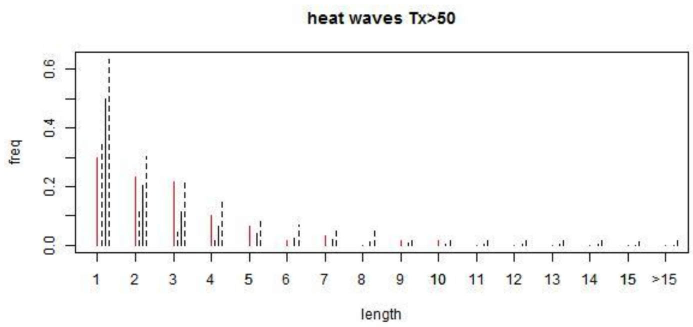

observations

simulations